African Journal of Advanced Pure and Applied Sciences (AJAPAS)
Online ISSN: 2957-644X
Volume 3, Issue 2, April-June 2024, Page No: 20-38
Website: *https://aaasjournals.com/index.php/ajapas/index*
معامل التأثير العربي 2023: (1.55) **SJIFactor 2023: 5.689** **ISI 2022-2023: 0.557**

An efficient Finite Shear Deformable Beam Element for Extensional-Bending Coupled Vibration of Antisymmetric Laminated Beams

Mohammed Ali Hjaji [1*], Hassan Mehdi Nagiar [2]
[1,2] Applied Mechanics Division, Mechanical and Industrial Engineering Department, University of Tripoli, Tripoli, Libya

[*]*Corresponding author: m.hjaji@uot.edu.ly*

Received: Febraury 02, 2024	Accepted: April 13, 2024	Published: April 19, 2024

Abstract
An exact one-dimensional finite beam element for extensional-bending coupled vibration analyses for antisymmetric composite laminated beams under various harmonic axial bending forces is developed in this study. The dynamic coupled equations and related boundary conditions are derived from Hamilton's variational principle. The formulation is based on Timoshenko beam theory and accounts for the effects of shear deformation caused by bending and translational and rotary inertia. It is also captured the effects of Poisson's ratio and structural extensional-bending coupling coming from composite material anisotropy. From the resulting coupled field equations, the closed form solutions are exactly obtained. A set of shape functions is then developed based on the exact solutions of the coupled equations and is utilized to formulate a finite beam element. The new beam element has two nodes with six degrees of freedom per node and successfully captures the coupled extensional-bending static and steady-state dynamic responses of antisymmetric composite laminate beams under harmonic forces. Several examples are performed for antisymmetric cross-ply and angle-ply laminated composite beams to investigate the effects of transverse shear deformation, and fiber orientation angle on coupled natural frequencies, quasi-static and steady state dynamic responses. Results based on the present finite element formulation are assessed and validated against other well-established finite element and exact solutions available in the literature.

Keywords: Exact Beam Element, Extensional-Bending Coupled Response, Antisymmetric Laminated Beams, Exact Shape Functions.

Cite this article as: M. A. Hjaji, H. M. Nagiar, "An efficient Finite Shear Deformable Beam Element for Extensional-Bending Coupled Vibration of Antisymmetric Laminated Beams," African Journal of Advanced Pure and Applied Sciences (AJAPAS), vol. 3, no. 2, pp. 20–38, April-June 2024.

عنصر عارضة فعال قابل لتشوه القص لاهتزاز الانحناء-المحوري المقترن لعارضات الرقائق المركبة الغير متماثلة

محمد علي الحجاجي[*1]، حسن المهدي النجار[2]
[2،1] شعبة الميكانيكا التطبيقية، قسم الهندسة الميكانيكية والصناعية، جامعة طرابلس، طرابلس، ليبيا

الملخص
تم تطوير عنصر محدود فعال أحادي البعد لعارضات ذات رقائق مركبة غير متماثلة من أجل التحليل الديناميكي للانحناء-المحوري المقترن والمعرضة قوى الانحناء المحورية التوافقية المختلفة. تم اشتقاق معادلات الحركة الحاكمة والشروط الحدودية ذات الصلة باستخدام صيغة هاملتون التغايرية. تعتمد المعادلات على نظرية العارضة لتيموشينكو وتفسر تأثيرات

تشوه القص الناجم عن الانحناء والقصور الذاتي الانتقالي والدوار. كما تم دراسة تأثير نسبة بوايسون والتشوه الحاصل من الانحناء-المحوري المقترن الناتج من تباين المواد المركبة. من معادلات الحاكمة المقترنة الناتجة، تم الحصول على الحل الدقيق للاستجابة الديناميكية للحالة المستقرة. وتم استخدامها لصياغة عنصر محدود الدقيق للعارضة. تم بعد ذلك تطوير مجموعة من دوال الاشكال بناءً على الحلول الدقيقة للمعادلات المقترنة والتي تم استخدامها لصياغة عنصر عارضة محدود. يحتوي عنصر العارضة الجديد على عقدتين مع ست درجات من الحرية لكل عقدة ويتحصل بنجاح على الاستجابات الديناميكية المقترنة ذات الانحناء-المحوري للحالة المستقرة لعارضات ذات الرقائق المركبة غير المتماثلة تحت تأثير القوى التوافقية المختلفة. تم إجراء العديد من الأمثلة على العارضات المركبة غير المتماثلة ذات الطبقات المتقاطعة والزاوية لدراسة تأثيرات تشوه القص المستعرض وزاوية توجيه الألياف على الترددات الطبيعية المقترنة والاستجابات الديناميكية شبه الثابتة والحالة المستقرة. يتم تقييم النتائج المستندة إلى تركيبة العناصر المحدودة الحالية والتحقق من صحتها مقابل العناصر المحدودة الأخرى الراسخة والحلول الدقيقة المتوفرة المنشورة سابقًا.

الكلمات المفتاحية: عنصر العارضة الدقيق، استجابة الانحناء-المحوري المقترن، عارضة رقائق مركبة غير متماثلة، دوال الاشكال الدقيقة.

1. Introduction

Composite laminated beams are experiencing growing utilization across diverse engineering applications owing to their impressive strength-to-weight and stiffness-to-weight ratios. Multilayered composite beams have found widespread use in aerospace, mechanical, and civil engineering. They serve as vital structural components in various applications such as aircraft wings, fuselage structures, helicopter blades, vehicle axles, propellant and turbine blades, as well as ship and marine structural frames, thanks to their outstanding features.

In various engineering applications, composite laminated beams often subjected to cyclic dynamic loading, such as harmonic excitations, arising from factors such as aerodynamic effects, hydrodynamic wave motion, wind loading, and imbalances in rotating or reciprocating machinery. These cyclic forces induce undesirable vibrations in composite laminated beams, they making them prone to fatigue failures. Consequently, fatigue failure considerations have gained significant importance in the design of composite laminated structural members. When subjected to harmonic forces, the transient component of dynamic response initially dominates but rapidly dampens out, thus having little importance in evaluating fatigue life. Conversely, the steady-state dynamic response is continued for a long term and is critical for evaluating fatigue life, and is the main focus of the present study. Thus, the study aims to develop an efficient finite beam element solution capable of isolating and capturing the steady-state dynamic response. Moreover, the present finite element solution is able to capture the quasi-static response and predict the eigen-frequencies and eigen-modes of the composite antisymmetric laminated beams.

2. Literature Review on Finite Element Formulations

While dynamic analysis of composite laminated antisymmetric beams using various beam theories has been extensively researched in recent years, many of these studies have focused only on the free vibrations of such composite beams. Numerous investigations have developed and examined the analytical exact solutions and finite element techniques specifically for the free vibration response of composite symmetric and antisymmetric laminated beams. But in this study, the literature review is focused only on the finite element solutions.

In general, the finite element solutions are based on three types of shape functions: (1) approximate polynomial interpolation functions, (2) shape functions based on the exact solution of the static equilibrium equations, and (3) shape functions based on the exact solution of the dynamic equations of motion. Finite element formulations based on the approximate shape functions are most common and are included in the works of Chandrashekhara and Bangera [1], Nabi and Ganesan [2], Bassiouni, etal. [3], Raveendranath, etal. [4], Palanivel [5], Vo and Inam [6], Elshafei [7], Vo etal. [8], Elmardi etal. [9], Talekara and Kotambkar [10], Horta etal. [11], and Kashani and Hashemi [12]. Based on higher-order shear deformation theory, Chandrashekhara and Bangera [1] used the conventional finite element to analyze the free vibration behavior of laminated composite beams by considering the effects of rotary inertia, Poisson's effect, and coupled extensional and bending deformations. Based on first-order shear deformation, Nabi and Ganesan [2] developed a finite element model to study the free vibration characteristics of composite laminated beams including the effects of shear deformation and bi-axial bending and torsion. Bassiouni, etal. [3] presented a finite element model to investigate the natural frequencies and mode shapes of laminated composite beams. Raveendranath, etal. [4] analyzed the composite laminated beams using a two-noded curved composite beam element with three degrees of freedom per node. The formulation incorporated Poisson's effect and the coupled flexural and extensional deformations together with transverse shear deformation. Palanivel [5] developed a two-noded C^1 finite element of eight degrees of freedom per node for flexural analysis of symmetric composite laminated beams. Vo and Inam [6] developed a two-noded C^1 finite beam element with five degrees of freedom per node to study the free vibration and buckling analyses of composite cross-ply laminated beams by using the refined shear deformation theory. Their formulations account for the parabolical

variation of the shear strains through the beam depth and all coupling coming from the material anisotropy. Elshafei [7] developed a finite element model based on the first order shear deformation theory to predict the static and free vibration analyses for isotropic and orthotropic beams with different boundary conditions and length-to-thickness ratios. Vo etal. [8] presented a finite element model based on sinusoidal shear deformation theory to study the free vibration and buckling of composite laminated beams with arbitrary lay-ups. They developed a two-noded C^1 beam element with five degree-of-freedom per node which accounts for shear deformation effects and all coupling effects coming from the material anisotropy. Elmardi etal. [9] formulated a finite element model to predict the free vibration characteristic of symmetric and antisymmetric layered composite beams. In their formulation, the effects of transverse shear deformation and rotary inertia were included. Talekara and Kotambkar (2020) developed a finite element model based on first order shear deformation theory to analyze the free vibration characteristic of the anisotropic composite beam. In their formulation, the effects of Poisson ratio, slenderness ratio, material anisotropy, lay-up angle and boundary conditions on the natural frequencies of laminated composite beams were investigated. Recently, Horta etal. [11] investigated the free vibration analysis of laminated composite beams using the finite element method, in which the two-noded Timoshenko beam element model formulated via strain gradient. More recently, based on finite element method with dynamic finite element techniques, Kashani and Hashemi [12] presented the free coupled bending-torsion vibration analysis of prestressed composite laminated beams subjected to static axial force and end moment. A feature common to the above finite element studies is use of approximate shape functions involving spatial discretization errors, and thus requiring fine meshes to converge to the actual solution.

Finite element solutions based on the exact solution of static equilibrium equations, include the words of Chakraborty et al. [13], Murthy et al. [14], and Hjaji etal. [15]. Based on the first order shear deformation theory, Chakraborty et al. [13] used the finite element to analyzed the free vibration and wave propagation in composite laminated beams having symmetric and asymmetric ply stacking. Based on higher-order shear deformation theory, Murthy et al. [14] formulated a refined two-node beam element for the axial-flexural-shear coupled vibration analysis in asymmetrically stacked composite beams. In their formulation, the shape functions used in the finite element are satisfied the static equilibrium governing equations. Hjaji etal. [15] developed a super-convergent finite beam element for open thin-walled beams with doubly symmetric cross-sections subjected to various twisting and warping moments. The proposed two-noded beam element having four degrees of freedom is based on shape functions which exactly satisfy the solution of the static equilibrium field equations. The formulation accounts for the shear deformation effects arising from warping and captures the torsional-warping coupled response of open thin-walled beams. Solutions based on the exact solution for static equilibrium equations have the advantage of avoiding locking problems, which could arise in some of the solutions based on polynomial interpolation.

Formulations based on the exact solution of the dynamic equations of motion include the works of Hjaji etal. [16, 17, 18, 19]. Hjaji etal. [16] formulated an exact finite beam element to investigate the dynamic analysis of torsional vibration of shafts under various harmonic twisting moments. The beam element developed has two-nodes with four degree of freedom is based on exact shape functions. A super-convergent finite beam element for the dynamic flexural response of symmetric laminated composite beams subjected to various harmonic bending forces is developed by Hjaji etal. [17]. Based on the assumptions of Timoshenko beam theory, a one-dimensional finite beam element with two-nodes and four degrees of freedom per element based on the exact shape functions is investigated. The new beam element is applicable to symmetric laminated composite beams and accounts for the effects of shear deformation, rotary inertia, Poison's ratio and fiber orientations. Recently, Hjaji etal. [18] developed an efficient finite beam element formulation for investigating the dynamic analysis of axially preloaded Euler-Bernoulli beams under harmonic bending excitations. The new finite beam element derived based on the shape functions exactly satisfy the solution of the governing bending field equation. More recently, Hjaji etal. [19] formulated an accurate and efficient finite beam element that depends on the exact shape torsional and warping deformation functions which exactly satisfied the solution of the governing coupled equations for open thin-walled beams with doubly symmetric cross-sections under various harmonic torsional and warping moments. The proposed beam element developed captures the effects of shear deformation due to non-uniform torsion, warping deformation and rotary inertial effects. The finite beam element solutions developed by Hjaji etal. [16, 17, 18, and 19] based on the exact solution of the dynamic equations of motion offer the following two advantages: (1) they eliminate discretization errors arising in conventional interpolation schemes and converge to the solution using a minimal number of degrees of freedom; and (2) they lead to beam elements that are free from shear locking.

Though a large number of finite element solutions studies dealing with the dynamic analysis of composite laminated beams are developed, it should be noted that no work is reported in the literature on dynamic analysis of antisymmetric laminated composite beams under various harmonic axial and bending forces using finite beam element formulation based on exact shape functions which exactly satisfy the solution of the dynamic equations

of motion. Thus, the aim of the present study is to develop such an efficient finite beam element solution based on the exact solutions. The formulation developed is accounts for the shear deformation effects caused by bending, translational and rotary inertias, Poison's ratio, fiber orientation, and extensional-bending coupling effects arising from the asymmetry of the cross section.

3. Kinematic Functions

A prismatic composite laminated beam having length L, thickness h and width b is considered as shown in Fig. (1). In the right-handed Cartesian coordinate system (X, Y, Z) defined on the mid-plane of the composite beam, the X axis aligns with the beam coordinate, $Y$and Z align with the principal axes of the cross-section. Since the cross-section of the composite beam have two axes of symmetry (i.e., Y and Z), therefore, the coupling between bending and torsion responses due to the section non-symmetry is disregarded. Consequently, the present study focused solely on the flexural behaviour in the $X-Z$ plane. Then, the displacement functions for a general point $p(x,z)$ of height z from the centroidal axis of composite beam based on the first order shear deformation theory are assumed to take the following form:

$$u_p(x,z,t) = u(x,t) + z\,\phi_x\,,\quad v_p(x,z,t) = 0\,,\quad \text{and}\quad w_p(x,z,t) = w(x,t) \tag{1-3}$$

in which $u(x,t)$ and $w(x,t)$ are the axial and transverse displacements of a point on the mid-plane in the X and Z directions, $u_p(x,z,t)$ and $w_p(x,z,t)$ are the axial and transverse displacement, respectively, $v_p(x,z,t)$ is the lateral displacement, and $\phi_x(x,t)$ is the rotation of the normal to the mid-plane about the Yaxis, where x and t are spanwise coordinate and time, respectively.

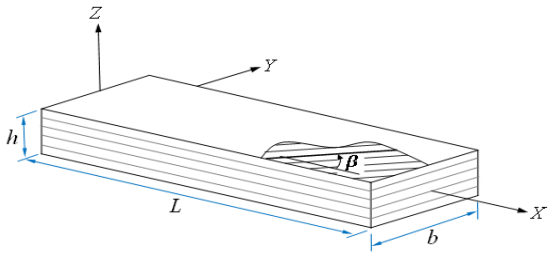

Figure (1): A composite laminated beam.

The normal and transverse strains of the composite laminated beam, as associated with the small-displacement theory of elasticity, are given as:

$$\varepsilon_x \approx \partial u_p/\partial x = \varepsilon_{xo} + z\,k_x\,,\quad \text{and}\quad \gamma_{xz} \approx \partial w_p/\partial x + \phi_x \tag{4}$$

where $\varepsilon_{xo} = \partial u/\partial x = u'$ is the mid-plane axial strain, $k_x = \partial\phi_x/\partial x = \phi_x'$ is the bending curvature, and the primes denote the differentiation with respect to x.

The laminated beam constitutive equations based on the first order shear deformation theory can be obtained by using the classical lamination theory to give:

$$\begin{Bmatrix} N_x \\ N_y \\ N_{xy} \\ M_x \\ M_y \\ M_{xy} \end{Bmatrix}_{6\times1} = \begin{bmatrix} A_{11} & A_{12} & A_{16} & B_{11} & B_{12} & B_{16} \\ A_{12} & A_{22} & A_{26} & B_{12} & B_{22} & B_{26} \\ A_{16} & A_{26} & A_{66} & B_{16} & B_{26} & B_{66} \\ B_{11} & B_{12} & B_{16} & D_{11} & D_{12} & D_{16} \\ B_{12} & B_{22} & B_{26} & D_{12} & D_{22} & D_{26} \\ B_{16} & B_{26} & B_{66} & D_{16} & D_{26} & D_{66} \end{bmatrix}_{6\times6} \begin{Bmatrix} \varepsilon_{xo} \\ \varepsilon_{yo} \\ \gamma_{xy} \\ k_x \\ k_y \\ k_{xy} \end{Bmatrix}_{6\times1} \tag{5}$$

where N_x, N_y and N_{xy} are the in-plane normal and shear forces, M_x, N_y and M_{xy} are the bending and twisting moments, $\varepsilon_{xo}, \varepsilon_{yo}$ and γ_{xy} are the mid-plane normal and shear strains, k_x, k_y and k_{xy} are the bending and twisting curvatures, respectively, A_{ij}, B_{ij} and D_{ij} denote the extensional, bending-extensional coupling and bending stiffnesses, respectively, and are expressed as functions of laminate ply orientation β and material properties as:

$$A_{ij}, B_{ij}, D_{ij} = \int_{-h/2}^{h/2} \left[\bar{Q}_{ij}\right](1, z, z^2)\,dz\,,\quad (\text{for } i,j = 1,2,6) \tag{6}$$

where $\bar{Q}_{ij}$ are the transformed reduced stiffnesses and are given by the following expressions [12]:

$$\bar{Q}_{11} = Q_{11}\,c^4 + 2(Q_{12} + 2Q_{66})\,s^2c^2 + Q_{22}\,s^4\,,\quad \bar{Q}_{12} = (Q_{11} + Q_{22} - 4Q_{66})\,s^2c^2 + Q_{12}(s^4 + c^4)$$

$$\bar{Q}_{22} = Q_{11}\,s^4 + 2(Q_{12} + 2Q_{66})\,s^2c^2 + Q_{22}\,c^4\,,\quad \bar{Q}_{16} = (Q_{11} - Q_{12} - 2Q_{66})\,s\,c^3 + (Q_{12} - Q_{22} + 2Q_{66})\,s^3c$$

$$\bar{Q}_{26} = (Q_{11} - Q_{12} - 2Q_{66})\,s^3c + (Q_{12} - Q_{22} + 2Q_{66})\,s\,c^3$$

$$\bar{Q}_{66} = (Q_{11} + Q_{22} - 2Q_{12} - 2Q_{66})\,s^2c^2 + Q_{66}(s^4 + c^4)$$

where β is the angle between the fiber direction and longitudinal axis of the composite laminated beam, $s = sin\beta$, $c = cos\beta$ (Fig. 1), and $Q_{11}, Q_{12},$ and Q_{22} are the stiffness constants and are given as:

$Q_{11} = E_{11}/(1 - \upsilon_{12}\upsilon_{21})$, $Q_{12} = \upsilon_{21}\, E_{11}/(1 - \upsilon_{12}\upsilon_{21}) = \upsilon_{12}\, E_{22}/(1 - \upsilon_{12}\upsilon_{21})$, and $Q_{22} = E_{22}/(1 - \upsilon_{12}\upsilon_{21})$

where E_{11}, E_{22} are Young moduli, and $\upsilon_{12}, \upsilon_{21}$are Poison ratios measured in the principal axes of the layer.

The present formulation is based on first order shear deformation theory in which the effect of transverse shear deformation due to bending is incorporated, then, the transverse shear force per unit length is given by [21]:

$$Q_{xz} = A_{55}\gamma_{xz} = A_{55}(\partial w/\partial x + \phi_x) = A_{55}(w' + \phi_x) \tag{7}$$

in which $A_{55} = k\int_{-h/2}^{h/2} \bar{Q}_{55}\, dz$, where $\bar{Q}_{55} = G_{13}c^2 + G_{23}s^2$, k is the correlation shear factor and is taken as 5/6 to account for the parabolic variation of the transverse shear stresses.

The composite laminated beam is subjected to dynamic axial force N_x and bending moment M_x, i.e., the lateral in-plane forces and moments in Ydirection are set to zero, $N_y = N_{xy} = M_y = M_{xy} = 0$. Thus, the constitutive equations for laminated beam based on the first order shear deformation theory are obtained by using the classical lamination theory as:

$$\begin{Bmatrix} N_x \\ M_x \end{Bmatrix}_{2\times1} = \begin{bmatrix} \overline{A}_{11} & \overline{B}_{11} \\ \overline{B}_{11} & \overline{D}_{11} \end{bmatrix}_{2\times2} \begin{Bmatrix} \varepsilon_{xxo} \\ k_x \end{Bmatrix}_{2\times1} = \begin{bmatrix} \overline{A}_{11} & \overline{B}_{11} \\ \overline{B}_{11} & \overline{D}_{11} \end{bmatrix}_{2\times2} \begin{Bmatrix} u' \\ \phi_x' \end{Bmatrix}_{2\times1} \tag{8}$$

where $\begin{bmatrix} \overline{A}_{11} & \overline{B}_{11} \\ \overline{B}_{11} & \overline{D}_{11} \end{bmatrix}_{2\times2} = \begin{bmatrix} A_{11} & B_{11} \\ B_{11} & D_{11} \end{bmatrix}_{2\times2} - \begin{bmatrix} A_{12} & A_{16} & B_{12} & B_{16} \\ B_{12} & B_{16} & D_{12} & D_{16} \end{bmatrix}_{2\times4} \begin{bmatrix} A_{22} & A_{26} & B_{22} & B_{26} \\ A_{26} & A_{66} & B_{26} & B_{66} \\ B_{22} & B_{26} & D_{22} & D_{26} \\ B_{26} & B_{66} & D_{26} & D_{66} \end{bmatrix}_{4\times4}^{-1} \begin{bmatrix} A_{12} & B_{12} \\ A_{16} & B_{16} \\ B_{12} & D_{12} \\ B_{16} & D_{16} \end{bmatrix}_{4\times2}$.

If the Poisson ratio effect is ignored, the coefficients $(\overline{A}_{11}, \overline{B}_{11}, \overline{D}_{11})$ in equation (8) are then replaced by the laminate stiffness coefficients (A_{11}, B_{11}, D_{11}), respectively.

4. Energy Expressions

Based on the first order shear deformation theory, the elastic strain energy U_s of the laminated composite beam is expressed as:

$$U_s = \frac{1}{2}\int_0^L [N_x\varepsilon_{xxo} + M_x k_x + Q_{xz}\gamma_{xz}]\, bdx = \frac{1}{2}\int_0^L [N_x u' + M_x\phi_x' + Q_{xz}(w' + \phi_x)]\, bdx$$

Substituting equations (5) and (7) into the above equation, obtains:

$$U_s = \frac{1}{2}\int_0^L [A_{11}u'^2 + 2B_{11}u'\phi_x' + D_{11}\phi_x'^2 + A_{55}(w'^2 + 2w'\phi_x + \phi_x^2)]\, bdx \tag{9}$$

The potential energy V of the applied dynamic forces are given as:

$$V = -\int_0^L [q_x(x,t)u(x,t) + q_z(x,t)w(x,t) + m_x(x,t)\phi_x(x,t)]\, bdx - [P_x(x_e,t)u(x_e,t)]_0^L - [P_z(x_e,t)w(x_e,t)]_0^L - [M_x(x_e,t)\phi_x(x_e,t)]_0^L \tag{10}$$

The kinetic energy T of the laminated composite beam is given by:

$$T = \frac{1}{2}\int_0^L \int_{-h/2}^{h/2} \rho\left[\dot{u}_p^2 + \dot{v}_p^2 + \dot{w}_p^2\right] bdzdx = \frac{1}{2}\int_0^L \left[I_1\dot{u}^2 + I_2\dot{w}^2 + 2I_2\dot{u}\,\dot{\phi}_x + I_3\dot{\phi}_x^2\right] bdx \tag{11}$$

where the densities I_1, I_2 and I_3 of the composite beam are introduced by:

$$I_1, I_2, I_3 = \int_{-h/2}^{h/2} \rho\,[1, z, z^2]\, dz = \sum_{k=1}^{m} \rho_n[(z_k - z_{k-1}), (z_k^2 - z_{k-1}^2)/2\,, (z_k^3 - z_{k-1}^3)/3]$$

in which the dot denotes the derivative with respect to time, and ρ_n (for $n = 1,2,3$) are the mass densities of the k^{th} layers.

5. Harmonic Vibration Functions

The applied harmonic forces and moments functions are expressed as:

$$q_x(x,t), q_z(x,t), m_x(x,t) = [\bar{q}_x(x),\ \bar{q}_z(x),\ \bar{m}_x(x)]\, e^{i\Omega t}$$
$$P_x(x_e,t), P_z(x_e,t), M_x(x,t) = [\bar{P}_x(x),\ \bar{P}_z(x),\ \bar{M}_x(x)]\, e^{i\Omega t}\ ,\ \text{for}\ x_e = 0, L \tag{12}$$

where Ω is the circular exciting frequency of the applied forces, $i = \sqrt{-1}$ is the imaginary constant, $q_x(x,t)$ and $q_z(x,t)$ are the distributed axial and transverse harmonic forces, $m_x(x,t)$ is the distributed harmonic bending moment, $P_x(x_e,t)$ and $P_z(x_e,t)$ are the concentrated axial and transverse harmonic forces, $M_x(x_e,t)$ are the concentrated harmonic bending moments, all forces and moments are applied at beam ends $(x_e = 0, L)$.

Under the given applied harmonic forces, the steady state displacement functions are given as:

$$u(x,t), w(x,t), \phi_x(x,t) = [U(x),\ W(x),\ \Phi_x(x)]\, e^{i\Omega t} \tag{13}$$

where $U(x)$, $W(x)$, and $\Phi_x(x)$ are the amplitudes for axial translation, transverse displacement, and bending rotation, respectively. As the present formulation aims to model solely the steady state dynamic response of the

structural composite laminated beam, the displacement functions proposed in equation (13) disregard the transient part of the dynamic response.

6. Governing Coupled Equations

The dynamic coupled equations for a composite antisymmetric laminated beam under harmonic forces can be obtained through Hamilton's principle, expressed as:

$$\int_{t_1}^{t_2} \delta(T - \Pi)\, dt = 0\,, \text{ for } \delta u(x,t)|_{t_1}^{t_2} = \delta w(x,t)|_{t_1}^{t_2} = \delta \phi_x(x,t)|_{t_1}^{t_2} = 0 \tag{14}$$

where t_1 and t_2 are two arbitrary time variables and δ denotes the first variation.

By substituting equations (11)-(13) into the energy expressions provided in equations (8)-(10), and subsequently integrating by parts, the resulting equations of motion are derived in matrix form as:

$$\begin{bmatrix} (I_1\Omega^2 + A_{11}\mathcal{D}^2) & 0 & (I_2\Omega^2 + B_{11}\mathcal{D}^2) \\ 0 & -(I_1\Omega^2 + A_{55}\mathcal{D}^2) & -A_{55}\mathcal{D} \\ (I_2\Omega^2 + B_{11}\mathcal{D}^2) & -A_{55}\mathcal{D} & (I_3\Omega^2 - A_{55} + D_{11}\mathcal{D}^2) \end{bmatrix}_{3\times3} \begin{Bmatrix} U(x) \\ W(x) \\ \Phi_x(x) \end{Bmatrix}_{3\times1} = \begin{Bmatrix} -\bar{q}_x(x) \\ \bar{q}_z(x) \\ \bar{m}_x(x) \end{Bmatrix}_{3\times1} \tag{15}$$

The associated boundary conditions are:

$$\begin{aligned} &[bA_{11}U'(x) + bB_{11}\Phi_x'(x) - \bar{P}_x(x)]_0^L\, \delta U(x)]_0^L = 0 \\ &[bA_{55}(W'(x) + \Phi_x(x)) - \bar{P}_z(x)]_0^L\, \delta W(x)]_0^L = 0 \\ &[bB_{11}U'(x) + bD_{11}\Phi_x'(x) - \bar{M}_x(x)]_0^L\, \delta\Phi_x(x)]_0^L = 0 \end{aligned} \tag{16}$$

where $\mathcal{D}$ is the differential operator, i.e., $\mathcal{D} \equiv d/dx\,, \mathcal{D}^2 \equiv d^2/dx^2$. The equations presented in (15) govern the coupled extensional-bending dynamic response of composite antisymmetric laminated beams under various harmonic forces. This study concentrates on deriving the exact closed-form solutions for the steady-state dynamic response governed by these coupled equations.

7. Exact Solutions for Displacement Fields

The exact solution to the extensional-bending coupled equations in (14) is attained by equating the right-hand side of the equations to zero., i.e. $\bar{q}_x(x) = \bar{q}_z(x) = \bar{m}_x(x) = 0$. Then, the solutions of the displacement functions are given as:

$$\langle \Psi(x) \rangle_{1\times3} = \langle U(x) \quad W(x) \quad \Phi_x(x) \rangle_{1\times3} = \langle C \rangle_{1\times3}\, e^{\lambda_i x}\,, \text{ for } i = 1,2,3,\ldots,6 \tag{17}$$

where $\langle \Psi(x) \rangle_{1\times3} = \langle U(x)\ W(x)\ \Phi_x(x) \rangle_{1\times3}$ is the vector of displacements, and $\langle C \rangle_{1\times3} = \langle c_{1,i} \quad c_{2,i} \quad c_{3,i} \rangle_{1\times3}$ is the vector of unknown constants. By substituting equation (17) into the equations in (15), and aiming for a non-trivial solution, the determinant of the bracketed matrix is equated to zero, resulting in a sixth-order polynomial equation given as:

$$p_4\lambda_i^6 + p_3\lambda_i^4 + p_2\lambda_i^2 + p_1 = 0 \tag{18}$$

where $p_1 = \Omega^4 I_1[\Omega^2(I_1I_3 - I_2^2) - I_1A_{55}]$,

$p_2 = \Omega^2[\Omega^2 I_1(I_1D_{11} + I_3A_{11} - 2I_2B_{11}) + A_{55}(I_1I_3\Omega^2 - I_2^2\Omega^2 - I_2A_{11}]$,

$p_3 = \Omega^2[I_1D_{11}(A_{55} + A_{11}) + I_3A_{11}A_{55} - I_1B_{11}^2 - 2I_2B_{11}A_{55})]$, and $p_4 = A_{55}(A_{11}D_{11} - B_{11}^2)$.

Equation (18) yields six unique roots, denoted as λ_i $(for\ i = 1,2,3,\ldots,6)$. Corresponding to each root λ_i, there exists a set of constants $\langle C \rangle_{i,1\times3} = \langle c_{1,i} \quad c_{2,i} \quad c_{3,i} \rangle_{i,1\times3}$. Upon back-substitution into the coupled system of equations in (18), one can establish relationships between constants $c_{1,i}$ and $c_{2,i}$ to constants $c_{3,i}$ through $c_{1,i} = G_{1,i}c_{3,i}$ and $c_{2,i} = G_{2,i}c_{3,i}$, where $G_{1,i} = -(B_{11}\lambda_i^2 + I_2\Omega^2)/(A_{11}\lambda_i^2 + I_1\Omega^2)$, and $G_{2,i} = -A_{55}\lambda_i/(A_{55}\lambda_i^2 + I_1\Omega^2)$.

The exact solutions for extensional displacement $U(x)$, flexural displacement $W(x)$ and associated bending rotation $\Phi_x(x)$ are given in matrix form as:

$$\{\Psi(x)\}_{3\times1} = \left[\overline{G}\right]_{3\times6}[E(x)]_{6\times6}\left\{\overline{C}\right\}_{6\times1} \tag{19}$$

where $\left[\overline{G}\right]_{3\times6} = \begin{bmatrix} \begin{Bmatrix} G_{1,1} \\ G_{2,1} \\ 1 \end{Bmatrix} & \begin{Bmatrix} G_{1,2} \\ G_{2,2} \\ 1 \end{Bmatrix} & \cdots\cdots & \begin{Bmatrix} G_{1,6} \\ G_{2,6} \\ 1 \end{Bmatrix} \end{bmatrix}_{3\times6}$, $[E(x)]_{6\times6}$ is a diagonal matrix consisting of the exponential functions $e^{\lambda_i x}$ (for $i = 1,2,3,\ldots,6$), the vector of unknown constants $\langle \overline{C} \rangle_{1\times6} = \langle c_{3,1} \quad c_{3,2} \quad \cdots\cdots \quad c_{3,6} \rangle_{1\times6}$ is to be determined from the problem boundary conditions.

8. Finite Element Formulation

This section introduces a novel two-noded finite beam element developed for analyzing the extensional-bending coupled vibration of composite shear deformable antisymmetric laminated beams subjected to different harmonic axial and bending forces. Figure (2) shows the proposed two-noded finite composite beam element of length l_e and six degrees of freedom per element. To exactly investigate the solution of dynamic coupled field equations, a

set of shape functions is utilized, ensuring exact formulation of stiffness and mass matrices, along with the load potential vector.

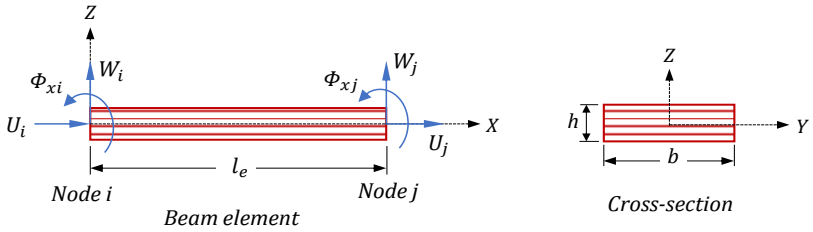

Figure (2): Two-noded beam element for extensional-bending coupled response.

In the present finite element formulation, the vector containing unknown integration constants is represented using nodal displacements $\langle d_n \rangle_{1\times6} = \langle U_1 \quad W_1 \quad \Phi_{x1} \quad U_2 \quad W_2 \quad \Phi_{x2} \rangle_{1\times5}$by applying the conditions $U(0) = U_1$, $W(0) = W_1$, $\Phi_x(0) = \Phi_{x1}$, $U(l_e) = U_2$, $W(l_e) = W_2$, and $\Phi_x(l_e) = \Phi_{x2}$, yields:

$$\{d_n\}_{6\times1} = \begin{Bmatrix} \{\Psi(0)\}_{3\times1} \\ \{\Psi(l_e)\}_{3\times1} \end{Bmatrix}_{6\times1} = \begin{Bmatrix} \{\Psi(0)\}_{3\times1} \\ \{\Psi(l_e)\}_{3\times1} \end{Bmatrix}_{6\times1} \begin{bmatrix} [\overline{G}]_{3\times6}[E(0)]_{6\times6} \\ [\overline{G}]_{3\times6}[E(l_e)]_{6\times6} \end{bmatrix}_{6\times6} \{\overline{C}\}_{6\times1} = [\mathcal{R}]_{6\times6}\{\overline{C}\}_{6\times1} \tag{20}$$

From equations (19) and (20), one obtains:

$$\{\Psi(x)\}_{3\times1} = [\overline{G}]_{3\times6}[E(x)]_{6\times6}[\mathcal{R}]^{-1}_{6\times6}\{d_N\}_{6\times1} = [H(x)]_{3\times6}\{d_N\}_{6\times1} \tag{21}$$

The matrix of shape functions for the extensional-bending coupled response is defined as $[H(x)]_{3\times6} = [\overline{G}]_{3\times6}[E(x)]_{6\times6}[\mathcal{R}]^{-1}_{6\times6}$. It is evident from equation (21) that the derived shape functions exactly satisfy the homogeneous solution of the coupled field equations presented in equation (15). Additionally, they are depending upon the beam element span, cross-section geometry, and the exciting frequency of the applied harmonic forces.

8.1 Energy Expressions in Terms of Nodal Displacements

The variations of the energy expressions for the composite antisymmetric laminated beam are, respectively, obtained in terms of nodal degrees of freedom as:

$$\delta T = \langle d_N \rangle_{1\times6}\left[\rho\Omega^2 \int_0^{l_e}([H(x)]^T_{6\times3}[Z_m]_{3\times3}[H(x)]_{3\times6} + [H_c(x)]^T_{6\times3}[Z_c]_{3\times3}[H_e(x)]_{3\times6})\,dx\right]\{d_N\}_{6\times1}e^{i\Omega t} \tag{22}$$

$$\delta U_s = \langle \delta d_N \rangle_{1\times6}\left(\int_0^{l_e}\left[[H'(x)]^T_{6\times3}[Z_a]_{3\times3}[H'(x)]_{3\times6} + [H'(x)]^T_{6\times3}[Z_S]_{3\times3}[H'_s(x)]_{3\times6} + [H_r(x)]^T_{6\times3}[Z_r]_{3\times3}\left[H_p(x)\right]_{3\times6}\right]dx\right)\{d_N\}_{6\times1}e^{i\Omega t} \tag{23}$$

and, $$\delta V = -\langle \delta d_N \rangle_{1\times6}\left(\int_0^{l_e}\left[[H(x)]^T_{6\times3}\{Q_d\}_{3\times1}dx + [[H(x)]^T_{6\times3}\{Q_c\}_{3\times1}\right]_0^{l_e}\right)e^{i\Omega t} \tag{24}$$

where $[Z_m]_{3\times3} = diag.[\rho I_1 b \quad \rho I_1\, b \quad \rho I_3 b]_{3\times3}$, $[Z_c]_{3\times3} = diag.[\rho I_2 b \quad 0 \quad \rho I_2 b]_{3\times3}$, $[Z_a]_{3\times3} = diag.[bA_{11} \quad bA_{55} \quad bD_{11}]_{3\times3}$, and $[Z_S]_{3\times3} = diag.[bB_{11} \quad bA_{55} \quad bB_{11}]_{3\times3}$, $[Z_r]_{3\times3} = diag.[0 \quad 0 \quad bA_{55}]_{3\times3}$, $[H_c(x)]^T_{6\times3} = [H_{1,j}(x) \quad 0 \quad H_{3,j}(x)]^T_{6\times3}$, $[H_e(x)]_{3\times6} = [H_{3,j}(x) \quad 0 \quad H_{1,j}(x)]_{3\times6}$, $[H'_s(x)]_{6\times3} = \left[\{H'_{3,j}(x)\}_{6\times1} \quad \{H_{3,j}(x)\}_{6\times1} \quad \{H'_{1,j}(x)\}_{6\times1}\right]^T_{6\times3}$, $[H_r(x)]^T_{6\times3} = \left[0 \quad 0 \quad \{H_{3,j}(x)\}_{6\times1}\right]^T_{6\times3}$, and $\left[H_p(x)\right]_{3\times6} = \left[0 \quad 0 \quad \{H'_{2,j}(x) + H_{3,j}(x)\}_{6\times1}\right]_{3\times6}$.

8.2 Discretized Equilibrium Equations

By substituting equations (22-24) into Hamilton's principle as depicted in equation (14), yields:

$$([K_e]_{6\times6} - \Omega^2[M_e]_{6\times6})_{6\times6}\{d_N\}_{6\times1} = \{F_e\}_{6\times1} \tag{25}$$

in which, the element stiffness matrix $[K_e]_{6\times6}$ is obtained as:

$$[K_e]_{6\times6} = \int_0^{l_e}\left[[H'(x)]^T_{6\times3}[Z_a]_{3\times3}[H'(x)]_{3\times6} + [H'_s(x)]^T_{6\times3}[Z_S]_{3\times3}[H'(x)]_{3\times6} + [H_r(x)]^T_{6\times3}[Z_r]_{3\times3}[H(x)]_{3\times6}\right]dx$$

The mass matrix $[M_e]_{6\times6}$ for the beam element is obtained as:

$$[M_e]_{6\times6} = \int_0^{l_e}[H(x)]^T_{6\times3}[Z_m]_{3\times3}[H(x)]_{3\times6}dx$$

while, the element load vector of the applied harmonic forces is given by:

$$\{F_e\}_{6\times1} = \int_0^{l_e} [[H(x)]^T_{6\times3}\{Q_d\}_{3\times1}dx \quad + [[H(x)]^T_{6\times3}\{Q_c\}_{3\times1}]_0^{l_e}$$

The provided formulations detail the elastic stiffness, mass matrices, and load vector designed for a one-dimensional, two-noded antisymmetric composite laminated beam element featuring three degrees of freedom per node. This proposed beam element is developed for investigating the steady-state dynamic analysis, particularly focusing on extensional-bending coupled responses by using the exact shape functions developed in this formulation. Although the mainly aimed at dynamic responses of composite laminated beams, the developed beam element can also be employed to capture quasi-static responses. Moreover, it facilitates the prediction of extensional-bending natural frequencies and associated mode shapes.

9. Numerical Examples and Discussions

The proposed one-dimensional finite beam element, developed within this study, aims to analyze the dynamic extensional-bending coupled response of composite antisymmetric laminated beams subjected to various harmonic bending forces and moments. It serves the following purposes:

- Establishing the steady-state dynamic coupled responses for antisymmetric laminated beams under harmonic bending forces and moments at a certain exciting frequency Ω.
- Capturing the quasi-static responses of composite antisymmetric laminated beams under given harmonic forces by utilizing very low exciting frequencies Ω compared to the first natural frequency of the composite beam ($\Omega \approx 0.01\omega_1$), where ω_1 represents the first natural frequency of the given composite beam.
- Predicting the natural frequencies and associated mode shapes of the given composite antisymmetric laminated beams under various harmonic forces.

In order to assess the accuracy and suitability of the proposed finite composite beam element formulated in this study, several numerical examples are presented. These examples investigate the extensional-bending coupled responses of antisymmetric laminated beams, considering different harmonic bending forces and moments under varying boundary conditions. The finite beam element under consideration based on the exact shape functions derived from the exact solutions of the governing coupled field equations of antisymmetric composite laminated beams. These shape functions are employed in formulating the mass, stiffness matrices, and load vector. The proposed finite beam element based on the exact shape functions, presents two distinguished advantages: (a) It eliminates the discretization errors inherent in conventional interpolation functions and converges towards the excellent results while utilizing a minimal number of degrees of freedom. (b) It results in elements devoid of shear locking issues. Consequently, it is observed that results obtained by using a single finite beam element exhibit excellent agreement with those derived from the exact closed-form solution established in a previous study [24]. The nodal degrees of freedom results obtained from the present formulation are compared with those from established Abaqus finite element models and exact solutions found in the literature. Within the Abaqus finite element model, the shell S4R elements are employed to simulate the composite laminated beam. The shell S4R element has four nodes with six degrees of freedom per node (i.e., three translations and three rotations), and effectively captures the shear deformation and distortional effects of the beam cross-section.

9.1 Example (1): Antisymmetric Laminated Composite beam - Validation

To assess the accuracy and validity of the proposed finite beam element solution, a graphite-polyester composite beam of four-layered antisymmetric $(30^o/-60^o/30^o/-60^o)$ laminates The composite beam of length $L = 0.572m$, and rectangular cross-section (width $b = 25.40mm$ and thickness $h = 25.40mm$) is subjected to uniformly distributed harmonic transverse force $q_z(x,t) = 5.0e^{i\Omega t}\, kN/m$ as shown in Figure (3). All four layers have the same thickness and made of the same orthotropic composite material as: $E_{11} = 221.0Pa$, $E_{22} = 6.90GPa$, $G_{12} = 4.80GPa$, $G_{13} = 4.14GPa$, $G_{23} = 3.45Pa$, $\upsilon_{12} = 0.3$, and $\rho = 1550.1\ kg/m^3$. This example is offered to achieve the steady-state dynamic analysis aimed at predicting the natural extensional-bending frequencies. It focuses on the coupled extensional-bending behavior of the given composite lamented beams having different boundary conditions.

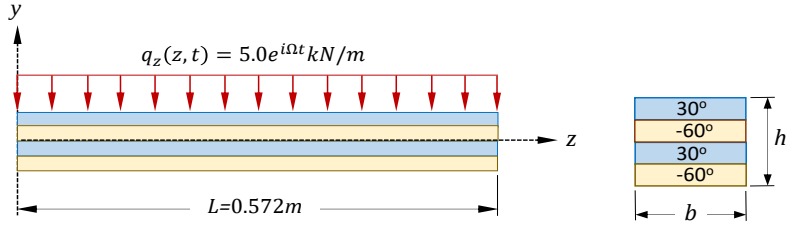

Figure (3): A composite antisymmetric laminated beam under harmonic distributed force.

In Abaqus finite element model, the composite antisymmetric beam is divided into 80 S4R shell elements along the longitudinal axis of the composite beam and 4 shell S4R elements along the beam width, i.e., a total of 320 S4R shell elements with 2830 degrees of freedom are required to achieve the required accuracy, whereas the finite-element solution developed in the present study based on exact shape functions is conducted using a single finite element with two nodes and six degrees of freedom per node for clamped-free beam while for other boundary conditions, two beam elements with nine degrees of freedom are used.

When the beam subjected to uniformly distributed harmonic bending force: $q_z(x,t) = 5.0e^{i\Omega t} kN/m$, the natural frequencies associated with the extensional-bending coupled response can be determined through the steady state dynamic analyses by varying the exciting frequency f from nearly zero to $2500Hz$ for clamped-free and $3500Hz$ for clamped-pinned boundary conditions. Figures (4a-c) and (5a-c) illustrate the nodal axial displacement U_n, transverse displacement W_n, and related bending rotation ϕ_{xn} at the midspan $(x = L/2)$ for clamped-free and clamped-pinned composite beams as a function of exciting frequency f. Peaks observed on the diagrams signify the resonance, providing insights into the natural frequencies of the given composite beams with clamped-free and clamped-pinned boundary conditions. Following this, the first six natural frequencies extracted from the peaks of Figs. (4) and (5) are listed in Table (1) for various boundary conditions.

To validate the accuracy of the present finite element formulation, the first six natural coupled extensional-bending frequencies predicted from the present formulation are compared with those reported by Jun et al. [21] and Abaqus finite shell element model. Remarkably, the present finite element solution demonstrates outstanding agreement with the findings presented by Jun et al. [21]. Consequently, the present solution accurately captures the eigen-frequencies of composite antisymmetric laminated beams having clamped-free, clamped-clamped, clamped-pinned, and pinned-pinned boundary conditions. Notably, the present finite element developed successfully exhibited that the fifth frequency in clamped-free and sixth frequency in clamped-pinned composite laminated beams are fully extensional natural frequencies. This leads to conclude that, the present finite beam element solution is successful at extracting the eigen-frequencies and eigen-modes of the given composite beams.

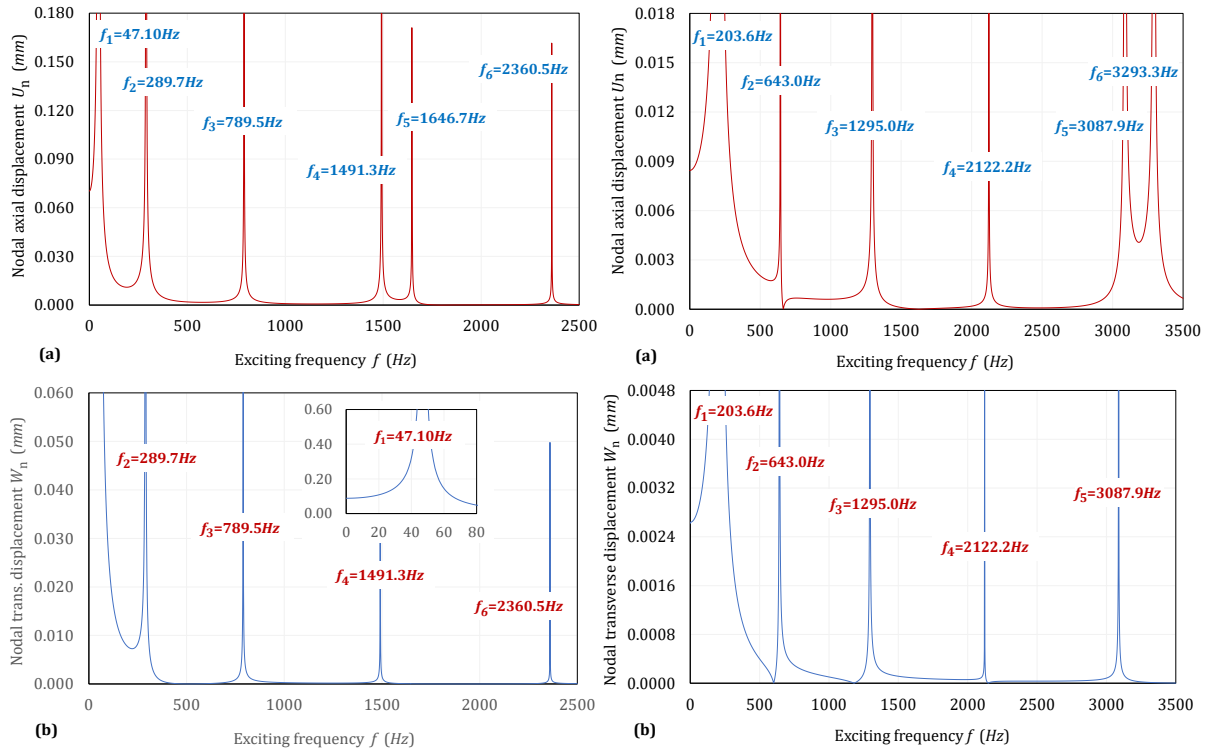

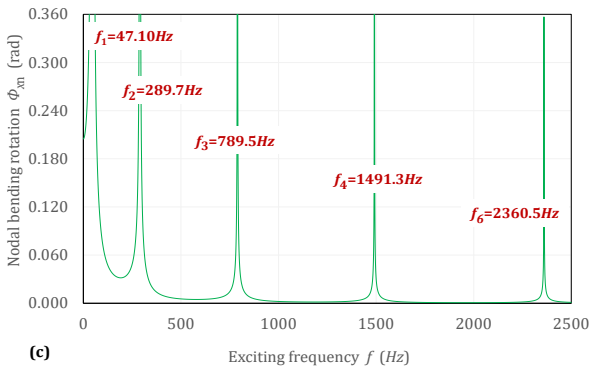

Figure (4): Natural frequencies of antisymmetric (30º/-60º/30º/-60º) laminated clamped-free beam

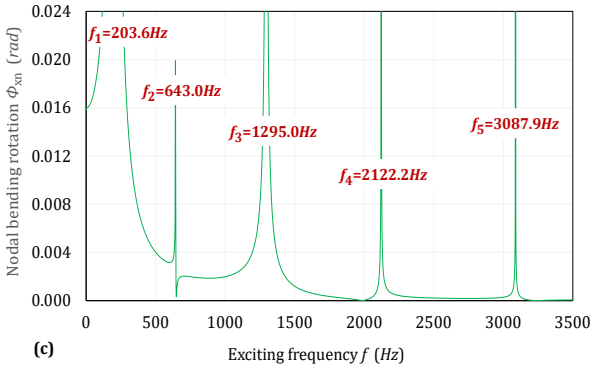

Figure (5): Natural frequencies of antisymmetric (30º/-60º/30º/-60º) laminated clamped-pinned beam

Table (1): Natural frequencies for composite antisymmetric (30º/-60º/30º/-60º) laminated beam.

Boundary condition	Frequency Number	Natural frequencies in (*Hz*)			%Difference =[2-1]/2	%Difference =[2-3]/2
		Jun etal. [21][1]	Abaqus FE[2]	Present FE[3]		
Clamped-free	1	47.01	47.64	47.05	1.32%	1.24%
	2	289.7	291.4	289.7	0.58%	0.58%
	3	789.5	788.0	789.5	-0.19%	-0.19%
	4	1491.3	1468.1	1491.3	-1.58%	-1.58%
	5	1646.6	1667.8	1646.7*	1.27%	1.27%
	6	2360.4	2300.9	2360.5	-2.59%	-2.59%
Clamped-clamped	1	291.9	296.3	291.9	1.48%	1.48%
	2	778.2	779.8	778.2	0.21%	0.21%
	3	1464.7	1447.3	1464.8	-1.20%	-1.21%
	4	2310.9	2251.3	2311.0	-2.65%	-2.65%
	5	3282.4	3157.0	3282.5	-3.97%	-3.98%
	6	3293.3	3322.7	3293.5	0.88%	0.88%
Clamped-pinned	1	203.6	205.9	203.6	1.12%	1.12%
	2	643.0	642.2	643.0	-0.12%	-0.12%
	3	1295.0	1269.1	1295.0	-2.04%	-2.04%
	4	2122.2	2070.3	2122.2	-2.51%	-2.51%
	5	3087.6	2997.0	3087.9	-3.02%	-3.03%
	6	3293.2	3321.7	3293.3*	0.86%	0.85%
Pinned-pinned	1	131.7	135.3	131.8	2.66%	2.59%
	2	516.8	511.4	516.9	-1.06%	-1.08%
	3	1129.4	1112.9	1129.5	-1.48%	-1.49%
	4	1933.0	1895.3	1933.3	-1.99%	-2.00%
	5	2890.0	2880.0	2890.0	-0.35%	-0.35%
	6	3292.5	3319.7	3292.7	0.82%	0.81%

* Fully extensional natural frequency

9.2 Example (2): Quasi-static and Dynamic Responses - Verification

In this example, an antisymmetric cross-ply $(0^o/90^o)$ laminated composite beam subjected to uniformly distributed transverse harmonic force $q_z(x,t) = 200e^{i\Omega t}N/m$ along the beam axis is analyzed using the finite beam element developed in this formulation. The composite beam has a rectangular cross-section of width b=25.4mm and height of h=25.4mm. The two-layers are of equal thickness and made of the same orthotropic material whose properties are: $E_{11} = 25.0GPa$, $E_{22} = 1.0GPa$, $G_{12} = G_{13} = 0.5E_{22}$, $G_{23} = 0.2E_{22}$, $\upsilon_{12} = 0.25$, and $\rho = 1389.2kg/m^3$.

To demonstrate the validity and accuracy of the proposed finite beam element for predicting the quasi-static and steady-state dynamic responses, the numerical results obtained are compared with the results available in the literature. The quasi-static and steady state dynamic responses for the composite beam are carried out for various span to thickness ratio *L*/*h*. The quasi-static analysis captured by using a very low exciting frequency (i.e., $\Omega \approx 0.01\omega_1$) related to the first natural frequency $\omega_1$of the given composite beam is compared with the corresponding results reported in Khdeir and Reddy [22], Chakraborty et al. [13], Vo and Thai [23], and Hjaji and Nagiar [24], while the steady-state dynamic response computed at exciting frequency $\Omega = 1.80\omega_1$ is compared with Abaqus finite element model, in which the S4R shell elements are used to model the composite beam.

In Abaqus finite element model, the composite beam subdivided into 80 S4R shell elements along the longitudinal axis of the beam and 2 S4R shell elements along the beam width which are needed to attain the required accuracy. The model consists of 160 S4R shell elements with six degrees of freedom per node, which leads to approximately 1460 degrees of freedom. While the finite element solution developed in the present study based on exact shape functions is conducted using two beam elements with three degrees of freedom per node (i.e., the model has only 9 degrees of freedom). It is noted to give results exactly matching with those based on the exact closed-form solution reported in Hjaji and Nagiar [24] up to five significant digits. This is a natural outcome of the fact that the present finite beam element is based on the shape functions, which exactly satisfy the exact solutions of the governing coupled field equations, which in turn eliminates discretization errors encountered in classical finite-element formulations.

9.2.1 Quasi-Static Analysis

To offer further comparison, the non-dimensional form of the transverse displacement function $\overline{W} = 100bh^3E_{22}w/q_zL^4$ defined by Vo and Thai [23] is investigated for the static analysis of composite beams under distributed harmonic transverse force. The quasi-static results of non-dimensional mid-span displacements $\overline{W}$ for different span-to-thickness ratio (*L*/*h*) obtained from the present finite beam element are compared with those results based on exact solutions of Khdeir and Reddy [22], and Hjaji and Nagiar [24], and finite element solutions provided by Chakraborty et al. [13], and Vo and Thai [23]. The effect of span-to-thickness ratio (*L*/*h*) on the static responses of the non-dimensional mid-span transverse displacements $\overline{W}(L/2)$ for antisymmetric $(0^o/90^o)$ laminated composite beams are provided in Table (2), for clamped-free and simply-supported boundary conditions. It is evident that the static results obtained from the present finite element formulation exhibit excellent agreement with those obtained from other solutions.

Table (2): Static results for non-dimensional mid-span displacement of antisymmetric (0°/90°) laminated beam under distributed harmonic transverse force.

Beam type	Reference	$\overline{W}(L/2)$			
		(*L*/*h*)=5	(*L*/*h*)=10	(*L*/*h*)=20	(*L*/*h*)=50
Clamped-free	Khdeir and Reddy [22]	16.436	12.579	-	11.345
	Chakraborty etal. [13]	16.496	12.579	-	11.345
	Vo and Thai [23]	16.461	12.604	11.640	11.370
	Hjaji and Nagiar [24]	16.448	12.591	11.626	11.357
	Present finite element	16.448	12.591	11.626	11.357
Simply supported	Khdeir and Reddy [22]	5.036	3.750	-	3.339
	Chakraborty etal. [13]	5.048	3.751	-	3.353
	Vo and Thai [23]	5.043	3.757	3.436	3.346
	Hjaji and Nagiar [24]	5.040	3.752	3.432	3.342
	Present finite element	5.040	3.752	3.432	3.342

The quasi-static nodal results for the axial displacement U_n, transverse displacement W_n, and the corresponding bending rotation Φ_{xn} (for *n*=1,2,…,6) depicted along the composite beam coordinate axis *x* for span-to-height ratio of $L/h = 50$, in the antisymmetric $(0^o/90^o)$ composite laminated beam having clamped-free and simply-supported boundary conditions, are demonstrated in Figs. (6a-c) and Fig.(7a-c) respectively. The present finite element solution is validated by comparison with those given in exact solution of Hjaji and Nagiar [24], and Abaqus finite shell element solution. Even though the present formulation efficiently computed the nodal results by using single element for clamped-free and two beam elements for simply-supported beam, but for the sake of comparison, five beam elements with a total 18 dof are utilized. Thus, the quasi-static nodal results obtained from the proposed finite beam element show excellent agreement with those results obtained by other two solutions. Therefore, the present finite beam element is able to efficiently capture the static response of the given composite beams by keeping the number of degrees of freedom a minimum.

9.2.2 Dynamic Analysis

The steady state dynamic results for the nodal axial displacement U_n, transverse displacement W_n, and the related bending rotation Φ_{xn} (for n=1,2,…,6) plotted against the beam axis x for clamped-free and simply-supported composite beams with span-to-height ratio $L/h = 50$, are shown in Fig. (6d-f) and Fig.(7d-f), respectively. Figures illustrate the nodal dynamic responses obtained from the three solutions and for three different values of exciting frequencies related to the first natural frequency, $\Omega_1 = 0.60\omega_1$, $\Omega_2 = 1.60\omega_1$, and $\Omega_3 = 2.60\omega_1$, where the first natural frequency for clamped-free beam is $f_1 = 29.04Hz$ and for simply-supported composite beam is $f_1 = 13.09Hz$. Three solutions, based on the exact solution of Hjaji and Nagiar [24], Abaqus finite shell solution and the finite beam element solution developed in this study are overlaid on the same diagrams for comparison. It is clear that the nodal dynamic results based on the three solutions are exactly coincided. In other words, the nodal steady state dynamic responses obtained from the present finite beam element using 18 dof demonstrate an excellent agreement with those results based on exact solution in Hjaji and Nagiar [24] and Abaqus finite shell element model having 1460 dof. Once more, the present finite beam element employing exact shape functions successfully achieves the steady state dynamic response, thereby eliminating the discretization errors commonly arise in traditional finite element formulations replying on the interpolated shape functions.

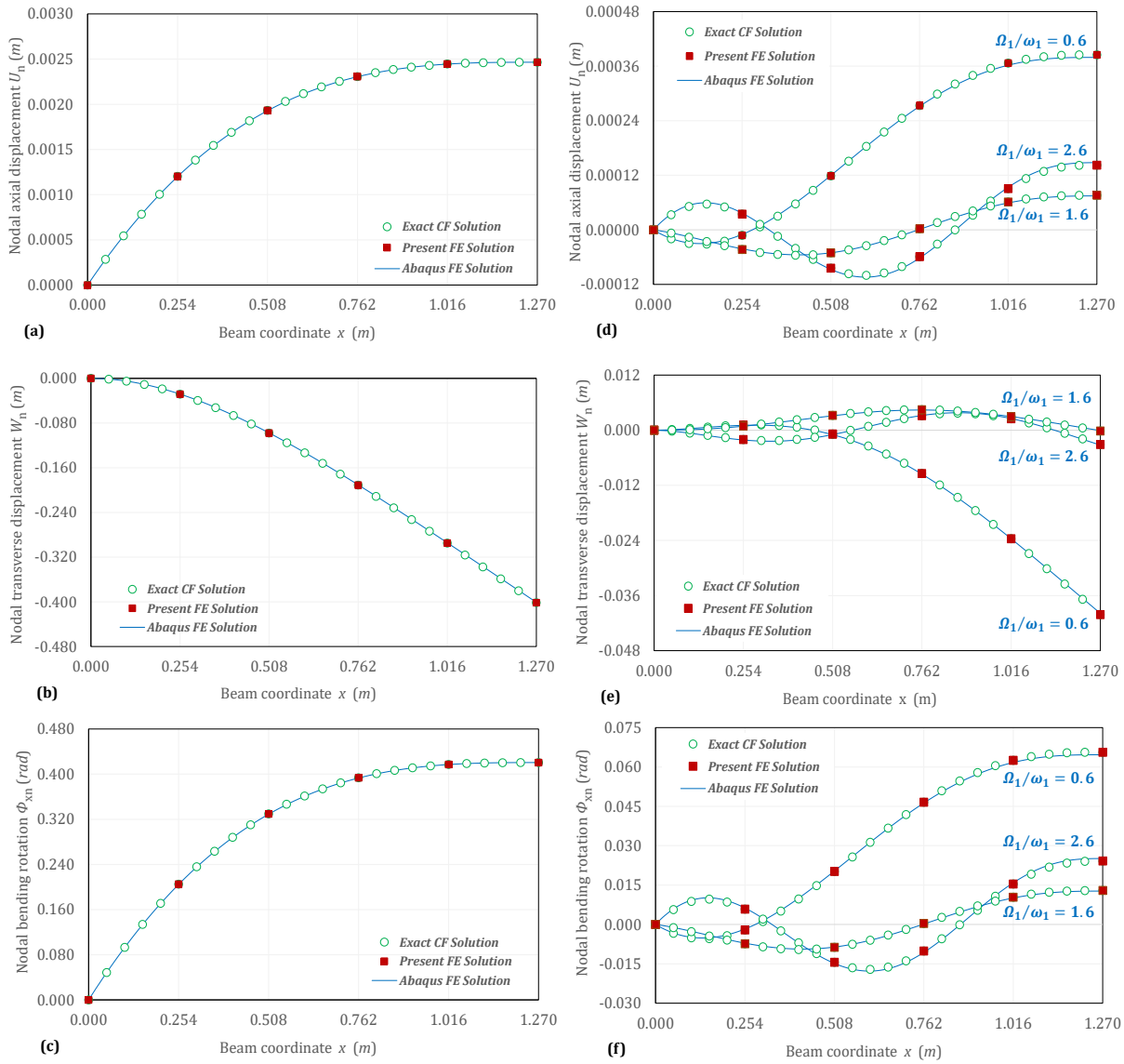

Figure (6): Quasi-static and dynamic responses of composite antisymmetric (0°/90°) laminated clamped-free beam under distributed transverse harmonic force (L/h=50).

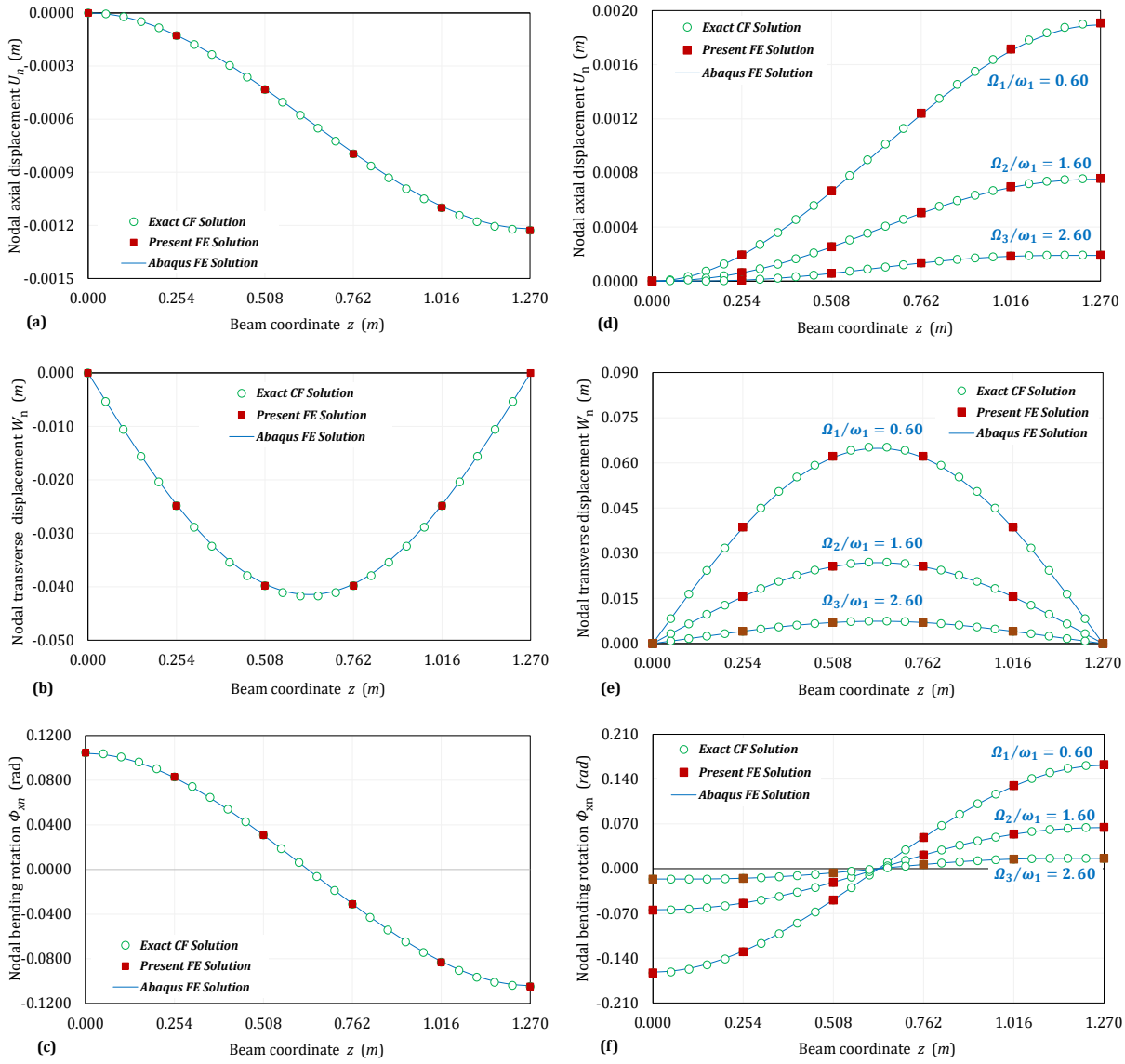

Figure (7): Quasi-static and dynamic responses of composite antisymmetric (0°/90°) laminated Simply-supported beam under distributed transverse harmonic force (L/h=50).

9.2.3 Fiber Orientation Effect on Static Response

In order to evaluate the convergence and accuracy of the proposed finite element solution to predict the static response of the composite beam, additional comparison is presented in Table (3). The influence of varying fiber orientation angle β on the dimensionless mid-span static nodal displacement $W_n(L/2)$ for antisymmetric composite $(0^o/\beta^o)$ laminated beam subjected to uniformly distributed harmonic transverse force. The composite beam is analyzed for different span-to-height ratio (L/h=5, 10, and 50) and for simply-supported, clamped-free, clamped-simply supported, and clamped-clamped boundary conditions. A comparison with the static results of Karamanli [25] demonstrates that the static results of the antisymmetric composite beam $(0^o/\beta^o)$ calculated from the present solution exhibits an excellent agreement. Again, the proposed finite beam element solution effectively captures the quasi-static response of the given composite laminated beams.

Table (3): Dimensionless mid-span static displacement of antisymmetric $[0^o/\beta^o]$ composite beams having various boundary conditions.

Boundary condition	Reference	Ratio (L/h)	Dimensionless mid-span static displacements of antisymmetric [0°/β°] composite beams for various boundary conditions						
			0°	15°	30°	45°	60°	75°	90°
Simply-supported	Karamanli [25]	5	1.8234	1.8910	2.1276	2.6757	3.7836	4.8467	5.0359
	Present FES		1.8238	1.8910	2.1276	2.6757	3.7836	4.8467	5.0359

	Karamanli [25]	10	0.9234	0.9726	1.1547	1.6169	2.6223	3.5968	3.7502
	Present FES		0.9238	0.9726	1.1549	1.6169	2.6227	3.5988	3.7502
	Karamanli [25]	50	0.6354	0.6787	0.8433	1.2780	2.2507	3.1969	3.3387
	Present FES		0.6356	0.6787	0.8433	1.2781	2.2508	3.1971	3.3389
Clamped-free	Karamanli [25]	5	5.7197	5.9398	6.7150	8.5326	12.245	15.812	16.436
	Present FES		5.7199	5.9398	6.7150	8.5365	12.245	15.812	16.436
	Karamanli [25]	10	3.0197	3.1844	3.7961	5.3561	8.7611	12.063	12.579
	Present FES		3.0204	3.1844	3.7961	5.3561	8.7611	12.063	12.579
	Karamanli [25]	50	2.1557	2.3027	2.8621	4.3397	7.6462	10.863	11.345
	Present FES		2.1559	2.3027	2.8621	4.3397	7.6464	10.863	11.345
Clamped-simply supported	Karamanli [25]	5	1.5899	1.6371	1.7929	2.1135	2.6811	3.2070	3.3197
	Present FES		1.5900	1.6368	1.7929	2.1130	2.6810	3.2070	3.3198
	Karamanli [25]	10	0.5983	0.6229	0.7107	0.9194	1.3500	1.7637	1.8345
	Present FES		0.5984	0.6229	0.7107	0.9194	1.3500	1.7637	1.8345
	Karamanli [25]	50	0.2636	0.2811	0.3475	0.5223	0.9125	1.2919	1.3490
	Present FES		0.2637	0.2811	0.3475	0.5223	0.9125	1.2919	1.3490
Clamped-clamped	Karamanli [21]	5	1.3247	1.3579	1.4634	1.6645	1.9954	2.3025	2.3786
	Present FES		1.3249	1.3579	1.4634	1.6645	1.9954	2.3025	2.3786
	Karamanli [25]	10	0.4247	0.4394	0.4904	0.6057	0.8341	1.0527	1.0929
	Present FES		0.4247	0.4394	0.4904	0.6057	0.8341	1.0527	1.0929
	Karamanli [25]	50	0.1367	0.1455	0.1790	0.2669	0.4625	0.6527	0.6815
	Present FES		0.1367	0.1455	0.1790	0.2669	0.4625	0.6527	0.6815

To further validate the present finite element approach, the variation of nodal static mid-plane displacement results given in Table (2) are plotted along the beam coordinate axis *x* for simply-supported, cantilever, clamped-simply supported and clamped-clamped boundary conditions as depicted in Figures (8a-d), respectively. The figures illustrate that the nodal static results obtained through the present formulation exactly coincide with those obtained from the Abaqus finite shell element model, thus exhibiting excellent agreement. Therefore, the proposed finite beam element solution is reliable and accurate.

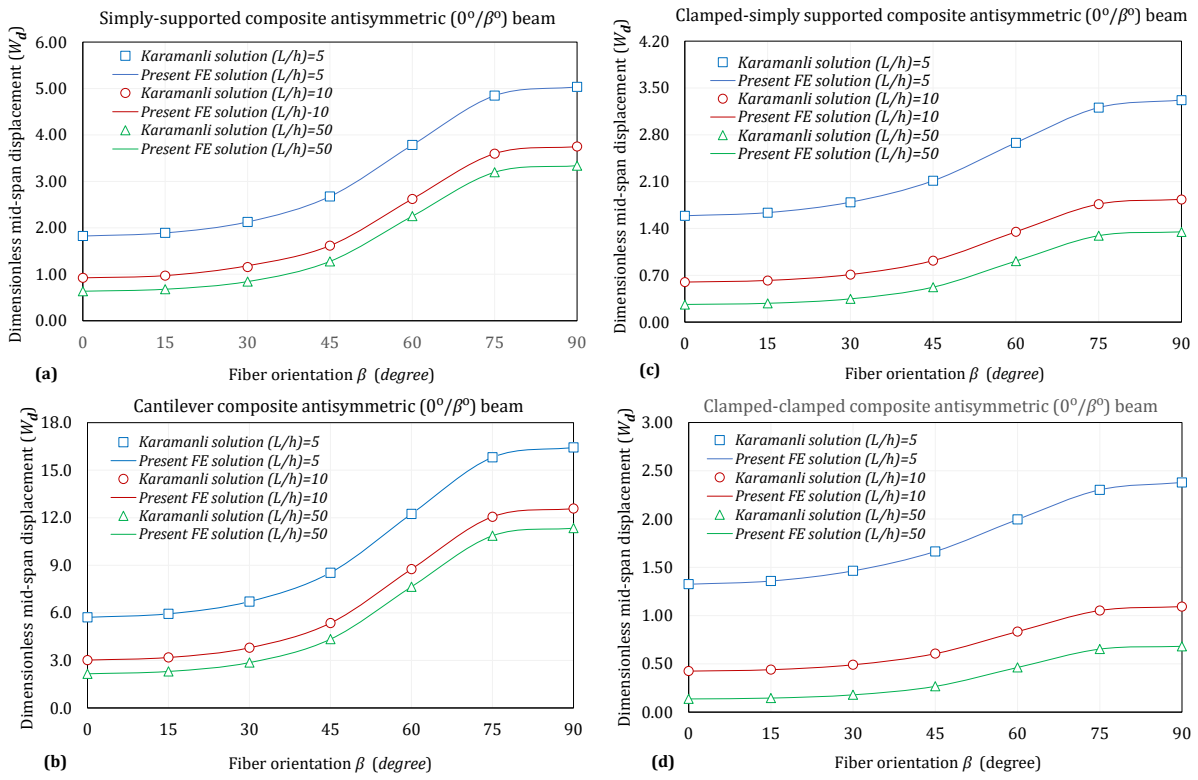

Figure (8): The static mid-span displacements versus fiber orientation β of antisymmetric $(0^o/\beta^o)$ beams under distributed harmonic transverse force for different boundary conditions.

9.2.4 Fiber Orientation Effect on Natural Frequencies

This section presents the variation of first four coupled natural frequencies (f_1, f_2, f_3 and f_4) with fiber orientation angle (β) of the composite antisymmetric ($0^o/\beta$) laminated clamped-free and clamped-simply supported beams having various span-to-height ratio L/h (10,20,30 and 40) as illustrated in Figs. (9) and (10), respectively. It is seen that, the natural frequencies of the antisymmetric composite beam are affected by the using different boundary conditions, fiber orientation angle, as well as L/h ratio. It is also noted that, the composite laminated beams of ($0^o/0^o$) fiber orientations have the highest coupled natural frequencies than the other fiber orientation angles, and consequently, because 100% of the fibers are oriented at longitudinal direction (i.e., $\beta = 0^o$) of the laminated beam. This causes the laminated beam to be more stiff than other fiber orientations. In addition, the influence of fiber orientation angles becomes more significant on the coupled natural frequencies when the fiber angles are observed up to around 60^o for cantilever boundary condition and 70^o for the case of clamped-simply supported boundary conditions. Furthermore, the composite laminated clamped-simply supported beam has larger natural frequencies than the composite cantilever beam.

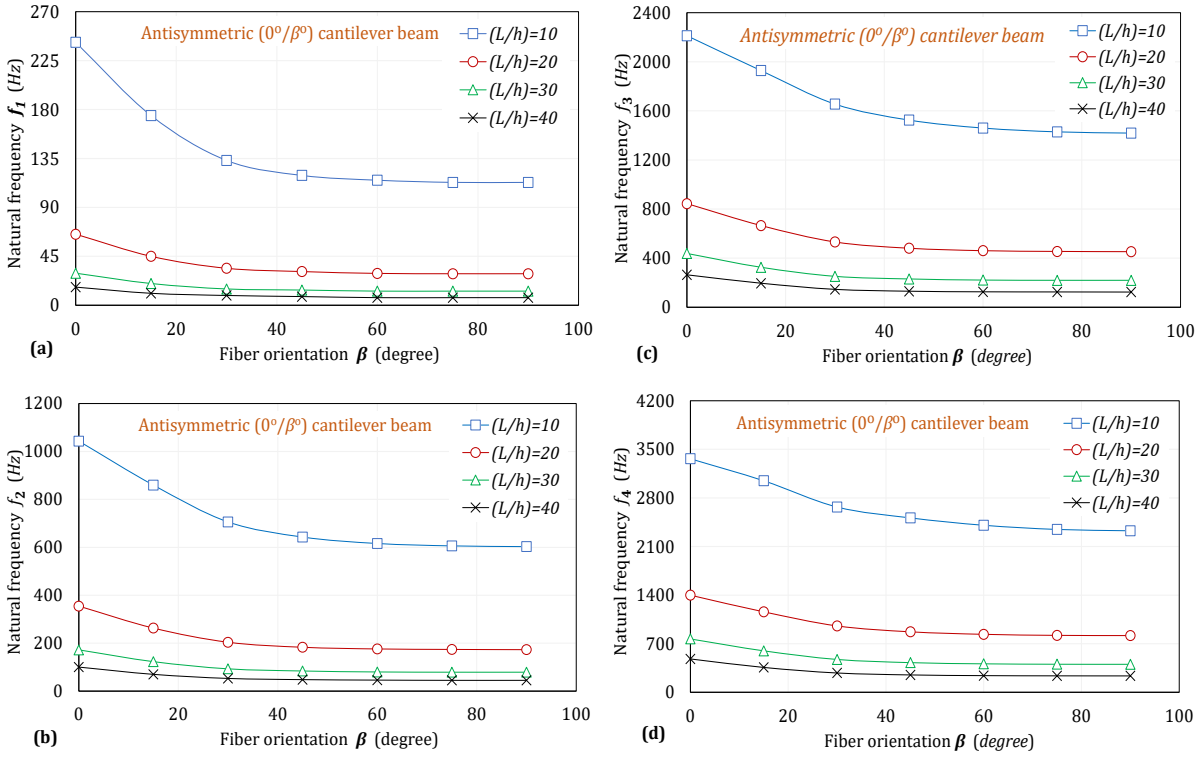

Figure (9): The variation of natural frequencies of antisymmetric ($0^o/\beta$) composite laminated cantilever beam for different (L/h) ratios versus fiber orientation/

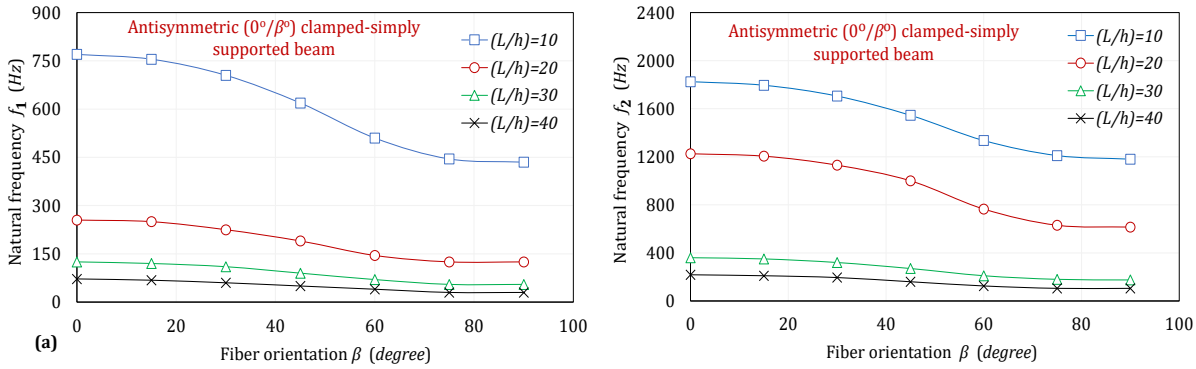

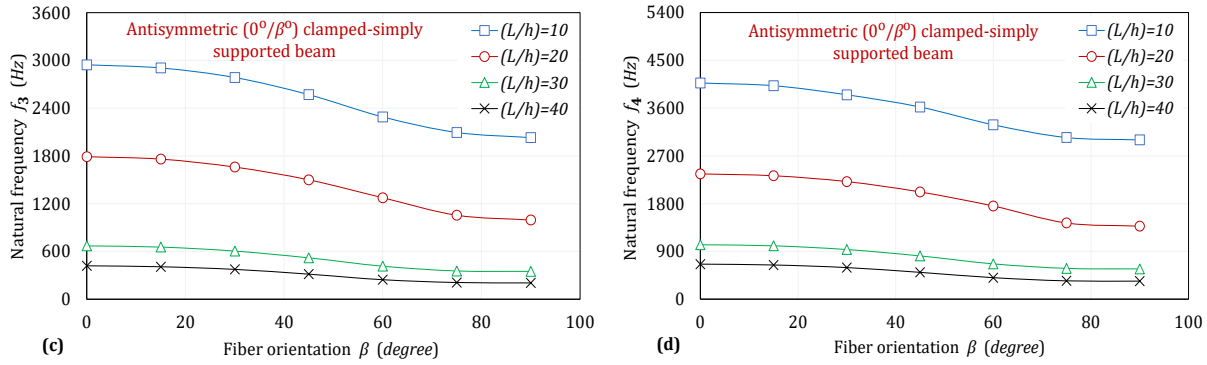

Figure (10): The variation of natural frequencies of antisymmetric ($0^o/\beta$) composite laminated clamped- simply supported beam having different (L/h) ratios versus fiber orientation.

9.3 Example (3): Asymmetric Laminated Beam under Harmonic forces

In this example, the accuracy of the proposed finite beam element is validated. For this purpose, a four-layered antisymmetric cross-ply $(0^o/90^o/0^o/90^o)$ laminated composite clamped-roller supported beam of 10m length (width b=40mm, and height h=40mm) subjected to distributed transverse harmonic forces $q_z(x,t) = 400e^{i\Omega t}\ N/m$, concentrated forces $P_{z1}(x,t) = 500e^{i\Omega t}N$, $P_{z2}(x,t) = 300e^{i\Omega t}N$ and $P_{z3}(x,t) = 200e^{i\Omega t}Nm$ is considered as shown in Figure (10). All four layers have the same thickness and made of the same orthotropic material properties: $E_{11} = 144.8\ GPa$, $E_{22} = 9.65\ GPa$, $G_{12} = G_{13} = 4.14\ GPa$, $G_{23} = 3.45\ GPa$, $\upsilon_{12} = 0.30$, and $\rho = 1750kg/m^3$. The example is given to achieve the following: (i) to compute the quasi-static response of the antisymmetric composite beam using very low exciting frequency $\Omega \approx 0.01\omega_1$, where the first natural frequency of the given composite beam is $f_1 = 2.56Hz$, and (ii) evaluate the steady state dynamic response of the given composite beam under harmonic forces at exciting frequency $\Omega = 100rad/sec$.

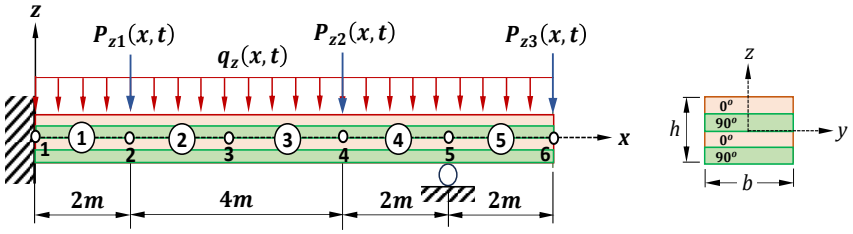

Figure (10): A composite antisymmetric laminated beam under various harmonic forces.

Two finite element solutions are provided for this problem. The first solution is based on the Abaqus finite shell element model, in which the antisymmetric composite beam is divided into 1000 shell S4R elements along the longitudinal axis of the beam, and 4 elements along the beam width. The composite beam model consists of 4,000 shell S4R elements with six degrees of freedom per node, which leads to approximately 30,000 degrees of freedom. The second solution is based on the present finite beam element, where the composite beam is subdivided into only five two-noded beam elements along the composite beam axis, i.e., the composite beam model has only 30 degrees of freedom.

The nodal axial displacement U_n, transverse displacement W_n, and bending rotation Φ_{xn}, are plotted against the beam coordinate axis as in Figs. (11a–c) for static response and Figs. (11d-f) for the steady-state dynamic response. The figures show excellent agreement between the nodal displacement functions predicted by the present finite beam element (using 30 degrees of freedom) and the Abaqus finite shell element model (using 30,000 degrees of freedom). The computational effort in the present finite element solution is several orders of magnitudes less than that of Abaqus finite element solution. This naturally occurs due to the fact that the proposed finite beam element is constructed using shape functions that exactly satisfy the solution of the governing extensional-bending coupled equations. As a result, this eliminates the discretization errors commonly encountered in finite element approaches.

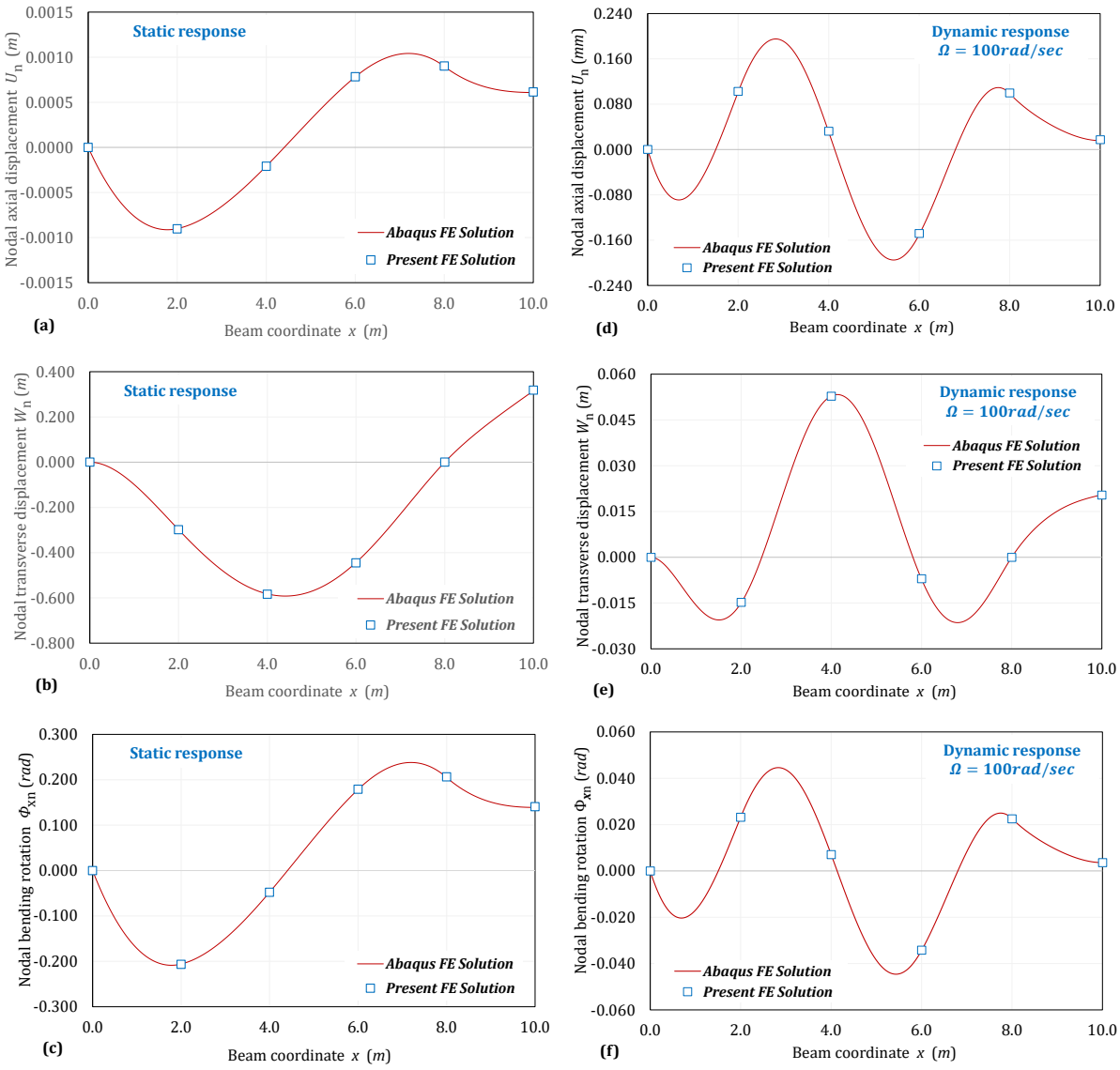

Figure (11): Static and dynamic responses of composite antisymmetric ($0^o/90^o/0^o/90^o$) laminated composite beam under various harmonic transverse forces.

10. Summary and Conclusions

- The equations governing the motion and corresponding boundary conditions of antisymmetric composite laminated beams subjected to different harmonic forces are formulated by applying the Hamiltonian variational principle.
- The formulation is based on the first-order shear deformation theory, which integrates the influences of shear deformation, rotary inertia, Poisson's ratio, and the interactions between extensional and bending deformations arising from material anisotropy.
- The new beam two-noded element is based on shape functions which exactly satisfy the solution of governing field equations and thus eliminates the discretization errors commonly found in other interpolation methods and generally exhibits excellent results while minimizing the number of degrees of freedom required.
- The new finite beam element successfully captures the extensional-bending coupled response of composite laminated beam with antisymmetric laminates.
- The proposed finite beam element effectively captures how composite beams respond to different harmonic forces in both static and steady state dynamics. It can obtain the steady state dynamic response without requiring eigen-modes extraction. Additionally, it has the ability to extract eigen-frequencies and eigen-modes when necessary.
- The present finite element solution offers excellent agreement with Abaqus finite shell element while requiring significantly less computational resources and modeling effort.

11. References

[1] Chandrashekhara, K. and Bangera, K.M., (1992), Free Vibration of Composite Beams Using a Refined Shear Flexible Beam Element, Computers and Structures, 43 (4), pp 719-727. doi:10.1016/0045-7949(92)90514-Z

[2] Nabi, S. M. and Ganesan, N., Generalized Element for the Free Vibration Analysis of Composite Beams, Computers and Structures, 51 (5), pp. 607-610. doi:10.1016/0045-7949(94)90068-X

[3] Bassiouni, A. S., etal. (1999), Dynamic analysis for laminated composite beams, Composite Structures, 44(2-3), pp 81-87. doi.org/10.1016/S0263-8223(98)00057-9

[4] Raveendranath, etal. (2000), Application of coupled polynomial displacement field to laminated beam elements, Computers and Structures, 78 (5), pp661-670. DOI:10.1016/S0045-7949(00)00054-7

[5] Palanivel, S. (2001), Flexural analysis of symmetric laminated composite beams using C^1 finite element, Computers and Structures, 54 (1), pp121-126. DOI:10.1016/S0263-8223(01)00066-6

[6] Vo, T., and Inam, F. (2012), Vibration and buckling of cross-Ply composite beams using refined shear deformation theory, 2nd International Conference on Advanced Composite Materials and Technologies for Aerospace Applications, Glyndŵr University, Wrexham, Uk, pp14-18.

[7] Elshafei, M. (2013), FE modeling and analysis of isotropic and orthotropic beams using first order shear deformation theory, Materials sciences and applications, 4, pp77-102. DOI: 10.4236/msa.2013.41010

[8] Vo, T.P., Thai, H., and Inam, F. (2013), Axial-flexural coupled vibration and buckling of composite beams using sinusoidal shear deformation theory, Archive of Applied Mechanics, 83(4), pp605-622. doi.org/10.1007/s00419-012-0707-4

[9] Elmardi, O.M., Algarray, A., and Mahdi, I.M. (2017), Free vibration analysis of composite laminated beams, International Journal of Engineering Research and Advanced Technology, 3(10), pp 9-25. http://dx.doi.org/10.7324/IJERAT.2017.3138

[10] Talekar, N. and Kotambkar, M. (2020), Free vibration analysis of generally layered composite beam with various lay-up and boundary conditions, Materials to-day-Proceedings, 21, pp1283–1292. DOI: 10.1016/j.matpr.2020.01.164

[11] Horta, T. and Filho, J. (2021), Free vibration of laminated composites beams using strain gradient notation finite element models, Materials research, 24(2), pp 1-14. doi.org/10.1590/1980-5373-MR-2021-0394

[12] Kashani, M.T. and Hashemi, S. M. (2022), On the free vibration and the buckling analysis of laminated composite beams subjected to axial force and end moment - A Dynamic Finite Element Analysis, Applied Mechanics, 3, pp 210–226.

[13] Chakraborty, A.D., etal. (2002), Finite element analysis of free vibration and wave propagation in asymmetric composite beams with structural discontinuities, Composite Structures, 55(1), pp 23-36. doi.org/10.1016/S0263-8223(01)00130-1

[14] Murthy, M.V., et al. (2005), A refined higher order finite element for asymmetric composite beams, Composite Structures, 67, pp 27–35. DOI: 10.1016/j.compstruct.2004.01.005

[15] Hjaji, M. A., etal. (2021), Exact finite beam element for open thin walled doubly symmetric members under torsional and warping moments, Journal of Structural Engineering and Applied Mechanics, 4 (4), pp 267-281. Doi. Org/10.31462/jseam.2021.04267281

[16] Hjaji, M. A. etal. (2016a), Exact finite element for torsional vibration of shafts under harmonic torsion, International Journal of Engineering Research and Technology (IJERT), 5 (9), pp 308-315.

[17] Hjaji, M. A., Nagiar, H. M., Allaboudi, E. G., and Kamour, A. (2016b), Super-convergent finite element for dynamic analysis of symmetric composite shear-deformable Beams under harmonic forces, Journal of Mechanical and Civil Engineering (IOSR-JMCE), 13(5), pp 06-17.

[18] Hjaji, M. A., etal. (2020), Exact finite element formulation for flexural vibration of axially pre-loaded Euler-Bernoulli beams, IOSR Journal of Mechanical and Civil Engineering, 7 (1), pp 52-64.

[19] Hjaji, M.A., etal. (2022), An efficient finite element of torsional dynamic analysis for open thin-walled beams under torsional excitations, Journal of Engineering Research, University of Tripoli, 34, pp 17-44.

[20] Jones, R. M. (1975), Mechanics of composite materials, McGraw-Hill, New York.

[21] Jun, L., Hongxing, H., and Rongying, S., (2008), A Dynamic stiffness approach for vibration analysis of a laminated composite beam, Science and Engineering of Composite Materials, 15, pp 285-302. doi.org/10.1016/j.ijmecsci.2007.09.014

[22] Khdeir, A., and Reddy, J. N. (1994), Free vibration of cross-ply laminated beams with arbitrary boundary conditions, International Journal of Engineering Science, 32, pp 1971-1980. doi.org/10.1016/0020-7225(94)90093-0
[23] Vo, T. and Thai, H., (2012), Static behavior of composite beams using various refined shear deformation theories. Composite Structures, 94 (8), pp 2513 - 2522. doi.org/10.1016/j.compstruct.2012.02.010
[24] Hjaji, M. A. and Nagiar, H. M., (2023), Analytical solution for dynamic analysis of asymmetric laminated composite shear-deformable beams, Journal of Applied Science, Sabratha University,11, pp 79-100.
[25] Karamanli, A. (2018), Bending analysis of composite and sandwich beams using ritz method, Anadolu University Journal of Science and Technology An-Applied Sciences and Engineering, 19(1), pp 10-23. DOI: 10.18038/aubtda.320144